

## Nanometric TiO<sub>2</sub> as NBBs for Functional Organic-inorganic Hybrids with Efficient Interfacial Charge Transfer

Gorbovyi P.,<sup>1</sup> Traoré M.,<sup>1</sup> Chhor K.,<sup>1</sup> Museur L.,<sup>2</sup> Kuznetsov A. I.,<sup>3</sup> Chichkov B. N.<sup>3</sup> and Kanaev A.<sup>1\*</sup>

<sup>1</sup>Laboratoire d'Ingénierie des Matériaux et des Hautes Pressions (UPR 1311), Institut Galilée, Université Paris 13, 93430 Villetaneuse - France; kanaev@limhp.univ-paris13.fr

<sup>2</sup>Laboratoires de physique des Lasers (UMR 7538), Institut Galilée, Université Paris 13, France

<sup>3</sup>Lazer Zentrum Hannover e.V., Germany

The purpose of this work is to establish a fabrication method for new electronic materials: organic-inorganic p-MAPTMS / titanium-oxo-alkoxy hybrids. The size-selected 5.2-nm TiO<sub>2</sub> nanoparticles (Nano Building Blocks - NBB) are generated in a sol-gel reactor with turbulent fluids micromixing. The surface exchange between propoxy and MAPTMS groups under vacuum pumping results in a stable nanoparticulate precursor available for laser-induced 2-photon polymerisation. The hybrids demonstrate quantum yield of photoinduced charges separation 6 % and can steadily trap photoinduced electrons at number density of 6% Ti atoms. The materials are suitable for 3D-microstructuring.

### 1. Introduction

Last decades organic-inorganic hybrid materials deserved a great interest. Many progresses have been achieved in synthesis of these materials and understanding of their physical properties (Gómez-Romero and Sanchez, 2003; rhari, 2009; Sanchez et al, 2010). Titanium dioxide hybrids attract particular interest due to a high refractive index, biocompatibility and electron transport properties. Direct writing of photonic structures was recently demonstrated using 2-photon femtosecond laser polymerisation in the TTIP-MAA (TTIP=titanium tetra-iso-propoxide; MAA=methacrylic acid) materials (Sakellari et al, 2009). Titanium oxide hybrids are also capable accumulating Ti<sup>3+</sup> centres useful in photochemical conversion and storage of solar energy (Cottineau et al, 2008a; Cottineau et al, 2008b).

Exceptional electronic properties of these hybrids are related to the inorganic component: TiO<sub>2</sub>. High electron-hole separation efficiency (below 16 %) has been reported in the TiO<sub>2</sub> colloids (Henglein, 1982). The absorption of photons results in the electron transition from the valence band (VB) formed by 2p-orbitals of O<sup>2-</sup> to the conduction band (CB) due to Ti<sup>4+</sup> 3d-orbitals (Daude et al, 1977). The high photosensibility is also observed in TiO<sub>2</sub> alcogels with charge separation efficiency of

about 25 % (Kuznetsov et al, 2005; Kuznetsov et al, 2006a). In our previous works, we have developed new photochromic PHEMA/TiO<sub>2</sub> based hybrids (pHEMA=Poly(2-hydroxyethyl methacrylate) with high charge separation efficiency of 12 % and electron loading capacity of 14% Ti atoms (Kameneva et al, 2005; Kuznetsov et al, 2006b; Kuznetsov et al, 2009). The charges separation and long-term storage is explained by the fact that VB holes rapidly escape into the organic component while CB electrons remain on the organic component as Ti<sup>3+</sup> polaron-like centres. We also observed a strong correlation between the photosensitivity and the material structure.

The elaboration process is crucial for the electronic properties of the electronic hybrid. A control of the inorganic-organic interface permits to improve the charge separation and further increase the material photosensitivity. The aim of this work is to propose an original elaboration process based on Nano Building Blocks (NBBs) approach, which consists in selective fabrication of titanium-oxo-alkoxy nanoparticles, surface exchange and their assembling into a polymer, which allows the material morphology control.

## 2. Materials and Methods

The synthesis schema by Kameneva et al (2005) has been generally adopted for the hybrid fabrication. However, the inorganic component morphology is poor defined in this approach with a generally broad size distribution. Because of that, substantially polydispersed samples are often subjected to analysis. To overcome this problem, we made use of the sol-gel reactor (Rivallin et al, 2005a; Rivallin et al, 2005b; Azouani et al, 2010). The reactor assures homogeneous reaction conditions in the mixed fluids and permits generation of monodispersed oxo-TiO<sub>2</sub> nanoparticles of different sizes (Azouani et al, 2007). Its main part is the T-mixer of Hartridge and Roughton type, which operates at high Reynolds numbers  $Re > 10^3$ . Two thermostatic stock solutions containing titanium tetra-iso-propoxide (TTIP) and water in solvent (2-propanol) are injected into the mixer through two input tubes. This injection is exocentric: two fluids form a vortex before entering the main tube. Two reagents flow rates are maintained equal and varying from 2 to 12 m/s by applying an external gas pressure (N<sub>2</sub>, purity 99.995 %). The diameters of two input (1.0 mm) and the main (2.0 mm) tubes are chosen for a continuity of the Reynolds number. The static T mixer performance has been studied by several groups and a considerable narrowing of the particle size distribution has been shown (Marchisio et al, 2006; Gradl et al, 2006; Marchisio et al, 2009). In application to the sol-gel process, its advantage is related to the hierarchical growth mechanism of the structural units, which reactivity stepwisely decreases with each size increase.

Our approach consists, first, in generation of diluted monodispersed TiO<sub>2</sub> nanocolloids in 2-propanol, followed by the solvent replacement by MAPTMS and increase of the nanocolloid concentration. In present experiments, the sol particles were generated with TTIP concentration  $C_{Ti} = 0.15$  M and hydrolysis ratio  $H = 2.0$  at 20 °C. According to Azouani and al. (2007), nanoparticles nucleate in these conditions; however, their growth is strongly prohibited. The reactor temperature was controlled by a thermostat *Haake, DC10K15*. TTIP of 98 % purity, 2-propanol (*Interchim*) and distilled water were used. A monomode optical fibre probe was developed to monitor in situ the

particle size ( $2R$ ) and the scattered light intensity ( $I$ ) of He-Ne laser by photon-correlated spectroscopy method, using a 16-bit, 255 channels PC board plugged digital correlator (*PhotoCor Instruments*). The observation volume defined by a mutual positioning of two monomode optical fibres is small enough ( $\approx 10^{-6} \text{ cm}^3$ ) to prohibit multiple scattering events. The measurements ( $I$ ,  $R$ ) were carried out in the automatic sampling mode with the data accumulation over 60 s, which permits rejection of nosy data due to rare dust particles, which prohibit observation of much smaller nanoparticles.

### 3. Results and Discussion

The autocorrelation function (ACF) of the produced  $\text{TiO}_2$  nanoparticles in 2-propanol is shown in figure 1a. The mean particle hydrodynamic radius of 2.60 nm is in agreement with previous measurements in similar experimental conditions (Azouani et al., 2007). At the humidity control, this size is stable on a long-time-scale exceeding a day, which explained by vanishing of the dominant contribution of oxolation reaction into the particles aggregation. The solvent exchange is carried out at the next stage. MAPTMS was preliminary distilled in order to eliminate impurities and traces of inhibitors of spontaneous polymerisation. The solvent exchange is performed by MAPTMS addition to the 2-propanol/ $\text{TiO}_2$  nanocolloid under stirring and vacuum pumping through LN trap overnight. The 2-propanol elimination has been validated by the Raman intensity decrease of the dominant symmetric CCC band situated at  $818 \text{ cm}^{-1}$  (Moran et al, 1998).

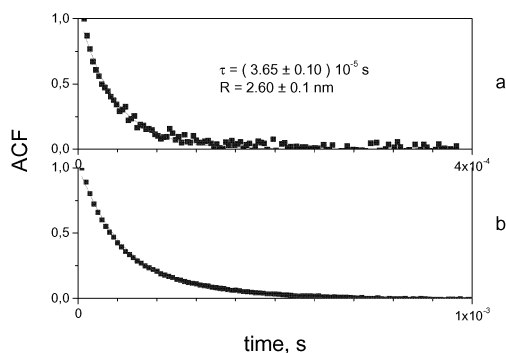


Figure 1: Characteristic ACFs of oxo- $\text{TiO}_2$  nanoparticles after preparation in the sol-gel reactor ( $[\text{Ti}] = 0.15 \text{ M}$ ,  $H=2$ ,  $T=20 \text{ }^\circ\text{C}$ , 2-propanol solution) (a) and after surface exchange with MAPTMS ( $C_{\text{Ti}} = 1.5 \text{ M}$ ) (b).

The solvent exchange does not influence the particles size and aggregation state, as this has been recently shown on pHEMA- $\text{TiO}_2$  hybrids (Gorbovyi et al., 2010). Figure 1b shows the ACF of the 1.5-M MAPTMS- $\text{TiO}_2$  colloid obtained after MAPTMS addition with the ratio of MAPTMS:2-propanol=1:10, which results in 10-times more concentrated colloids. Accordingly, the signal-to-noise ratio of the ACF (b) considerably improves compared to (a).

We have demonstrated in our previous work (Gorbovyi et al., 2011) that during the solvent exchange of 2-propanol with HEMA (2-hydroxyethyl methacrylate), a surface ligands replacement  $\text{OEMA} \rightarrow \text{O}^i\text{Pr}$  was possible. If the  $\text{O}^i\text{Pr}$  ligands replacement takes

place with MAPTMS, Si-O-Ti bounds have to be created. The vibration of these bounds ( $939\text{ cm}^{-1}$ ) does not appear in the FTIR spectra of the sol. The interaction between MAPTMS and the inorganic nanoparticles is not enough strong for covalent bonding. For this reason, the MAPTMS-TiO<sub>2</sub> hybrids seems to belong to the Class I hybrids according to the classifications proposed by Sanchez et al. (2010).

The polymerisation of the MAPTMS-TiO<sub>2</sub> precursor was realized both thermally with addition of the AIBN initiator and by 2-photon process using femtosecond near-IR laser (Ti-sapphire, 800 nm) with addition of a photoinitiator Irgacure 369. In the first case, non-coloured transparent hybrids were obtained after 24 hours heating at temperature at 75° C. The MAPTMS polymerization was monitored by Raman spectroscopy, observing characteristic vibrational peaks of C=C ( $1407\text{ cm}^{-1}$ ) and C=CH<sub>2</sub> ( $1641\text{ cm}^{-1}$ ) (Mabilleau et al., 2008). Figure 2 shows clearly that the intensity of the two C=C bands vanishes and, in the same time, the intensity of the C-C band at  $1455\text{ cm}^{-1}$  increases indicating the elongation of the polymeric chain. Our measurements show that some residual non-polymerised monomers remain in the hybrids with the increase of the nanoparticles loading.

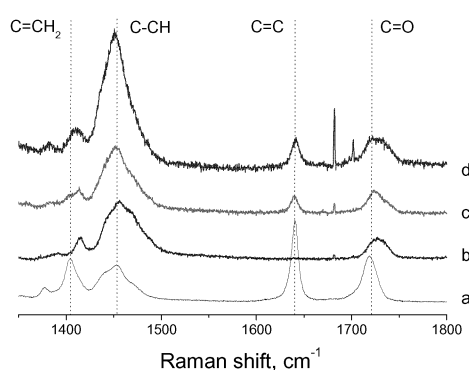


Figure 2: Raman Spectra of liquid MAPTMS-TiO<sub>2</sub> colloid  $C_{Ti}=1.5\text{ M}$  (a) and polymerised MAPTMS (b) and hybrids  $C_{Ti}=0.75\text{ M}$  (c) and  $C_{Ti}=3.0\text{ M}$  (d).

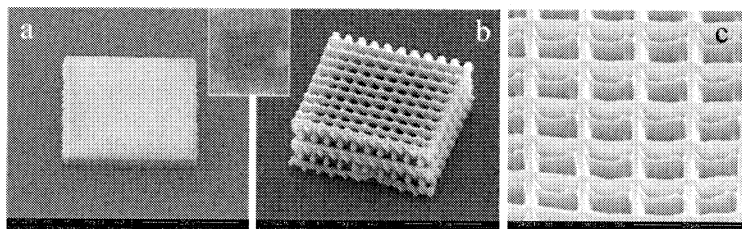


Figure 3: Microstructures achieved with laser-induced 2-photon polymerisation.

Figure 3 shows microstructuring obtained by laser-induced 2-photon polymerisation, which is a well-developed technique for nanostructuring of different photosensitive materials (Serbin et al., 2003, Farsary and Chichkov, 2009). Non-coloured transparent hybrids were obtained with different shapes and structure.

The as prepared hybrids darken when they are irradiated by UV light. This photochromism is related to a broadband visible absorption assigned to shallow polaronic  $Ti^{3+}$  centres formed by CB-electron trapping onto  $Ti^{4+}$ . The structured hybrids conserve their photochromism, which can be seen in the inset of figure 3, which shows the irradiated structure (rectangular parallelepiped) of figure 3a. We have measured the photonic sensitivity of the prepared hybrids in pump probe experiments using UV laser irradiation (Nd:Yag, 15 ps, 355 nm) with fluences of 10-80 mJ/cm<sup>2</sup>. Our present results (figure 4) evidence the photoinduced charge separation efficiency of the prepared samples,  $\eta = dN_{Ti^{3+}}/dN_{abs-ph} = 6\%$  and charges storage capacity of  $Q = N_{Ti^{3+}}/N_{Ti^{4+}} = 6\%$ . Compared to pHEMA-TiO<sub>2</sub> hybrids ( $\eta = 50\%$  et  $Q = 12\%$ ) (Gorbovyi et al., 2010), pMAPTMS-TiO<sub>2</sub> hybrids seem to be less efficient. This difference may be due to a lower hole affinity of the pMAPTMS polymer compared to pHEMA.

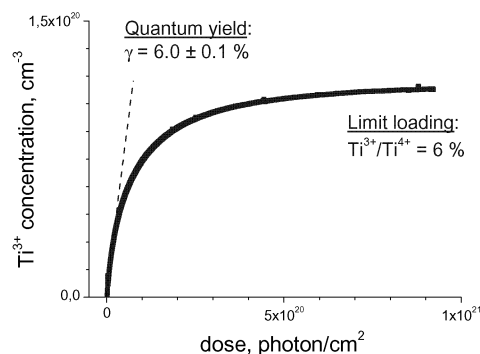


Figure 4: Darkening kinetics of MAPTMS-TiO<sub>2</sub> hybrids ( $C_{Ti} = 3.0\text{ M}$  or  $1.8 \cdot 10^{21}\text{ cm}^{-3}$ , sample thickness  $93\ \mu\text{m}$ ).

#### 4. Conclusion

We propose a new method of elaboration of electronic hybrid materials based on inorganic TiO<sub>2</sub> nanoparticle precursor. The key point is fabrication of size-selected titanium-oxo-alkoxy nanoparticles in a sol-gel reactor with turbulent fluids micromixing. The surface exchange between propoxy and polymerisable groups under vacuum pumping results in a stable nanoparticulate precursor available for both thermal and laser polymerisation. The p-MAPTMS/titanium-oxo-alkoxy hybrids show the quantum yield of photoinduced charges separation 6% and steadily trap photoinduced electrons at number density of 6%Ti atoms. 3D-laser microstructuring has been demonstrated in these materials. This proposed method allows a control of the electron transfer over the extended internal organic-inorganic interface and optimisation of the materials photosensitivity.

#### References

- Azouani R., Soloviev A., Benmami M., Chhor K., Bocquet J.-F., Kanaev A., 2007, J. Phys. Chem. C, 111-16243.

- Azouani R., Michau A., Hassouni K., Chhor K., Bocquet J.-F., Vignes J.-L., Kanaev A., 2010, *Chem Eng. Res. Design*, 88-1123.
- Cottineau T., Richard-Plouet M., Rouet A., Puzenat E., Sutrisno H., Piffard Y., Petit P.-E., Brohan L., 2008a, *Chem. Mater.*, 20-1421.
- Cottineau T., Brohan L., Pregelj M., Cevc P., Richard-Plouet M., Arcon D., 2008b, *Adv. Func. Mater.* 18-2602.
- Daude N., Gout C., Jouanin C., 1977, *Phys. Rev. B*, 15-3229.
- Fadeeva E., Koch J., Chichkov B., Kuznetsov A., Kameneva O., Bituyrin N., Sanchez C., Kanaev A., 2006, *Appl Phys A*, 84-27.
- Farsary M., Chichkov B. N., 2009, *Nature Phot.* 3-450.
- Gómez-Romero P., Sanchez C., *Functional Hybrid Materials*, 2003, Wiley, Weinheim.
- Gradl J., Schwarzer H. C., Schwertfirm F., Manhart M., Peukert W., 2006, *Chem. Eng. Proc.*, 45-908.
- Gorbovyi P., Uklein A., Tieng S., Traore M., Chhor K., Museur L., Kanaev A., *Nanoscale* (2011) in press.
- Henglein A., 1982, *Ber. Bunsenges. Phys. Chem.*, 86-241.
- Kameneva O., Kuznetsov A. I., Smirnova L. A., Rozes L., Sanchez C., Alexandrov A., Bituyrin N., Chhor K., Kanaev A., 2005, *J. Mater. Chem.*, 15-3380.
- Kuznetsov A. I., Kameneva O., Alexandrov A., Bituyrin N., Ph. Marteau, Chhor K., Sanchez C., Kanaev A., 2005, *Phys. Rev. E*, 71-021403.
- Kuznetsov A. I., Kameneva O., Alexandrov A., Bituyrin N., Ph. Marteau, Chhor K., Kanaev A., 2006a, *J. Phys. Chem. B*, 110-435.
- Kuznetsov A. I., Kameneva O., Rozes L., Sanchez C., Bituyrin N., Kanaev A., 2006b, *Chem. Phys. Lett.*, 429-523.
- Kuznetsov A. I., Kameneva O., Bituyrin N., Rozes L., Sanchez C., Kanaev A., 2009, *Phys. Chem. Chem. Phys.*, 11-1248.
- Mabilleau G., Cincu C., Basle M. F., Chappard D., 2008, *J. Raman Spectrosc.* 39-767.
- Marchisio D. L., Rivautella L., Barresi A. A., 2006, *AIChE J.*, 52-1877.
- Marchisio D. L., Omega F., Barresi A. A., 2009, *Chem. Eng. J.*, 146-456.
- Merhari L., Ed., 2009, *Hybrid Nanocomposite for Nanotechnology: Electronic, Optical, Magnetic and Biomedical Applications*, Springer, Limoges.
- Moran P. D., Bowmaker G. A., Cooney R. P., Finnie K. S., Bartlett J. R., Woolfrey J. L., 1998, *Inorg. Chem.*, 37-2741.
- Rivallin M., Benmami M., Gaunand A., Kanaev A., 2005a, *Chem. Phys. Lett.*, 398-157.
- Rivallin M., Benmami M., Kanaev A., Gaunand A., 2005b, *Chem. Eng. Res. Design*, 83-67.
- Sakellari I., Gaidukeviciute A., Giakoumaki A., Gray D., Fotakis C., Vamvakaki M., Farsari M., Reinhardt C., Ovsianikov A., Chichkov B.N., 2010, *Appl. Phys. A*, 100-359.
- Sanchez C., Rozes L., Ribot F., Laberty-Robert C., Grosso D., Sassoye C., Boissiere C., Nicole L.R., 2010, *Chimie*, 13-3.
- Serbin J., Egbert A., Ostendorf A., Chichkov B. N., Houbertz R., Domann G., Schulz J., Cronauer C., Frohlich L., Popall M., 2003, *Opt. Lett.*, 28-301.